Ablation of smooth muscle myosin heavy chain SM2 increases smooth muscle contraction and results in postnatal death in mice

Mei Chi[1], Yingbi Zhou[1], Srikanth Vedamoorthyrao, Gopal J. Babu, and Muthu Periasamy[2]

Department of Physiology and Cell Biology, College of Medicine and Public Health, Ohio State University, 304 Hamilton Hall, 1645 Neil Avenue, Columbus, OH 43210

Edited by Eric N. Olson, University of Texas Southwestern Medical Center, Dallas, TX, and approved October 14, 2008 (received for review August 19, 2008)

The physiological relevance of smooth muscle myosin isoforms SM1 and SM2 has not been understood. In this study we generated a mouse model specifically deficient in SM2 myosin isoform but expressing SM1, using an exon-specific gene targeting strategy. The SM2 homozygous knockout ($SM2^{-/-}$) mice died within 30 days after birth, showing pathologies including segmental distention of alimentary tract, retention of urine in renal pelvis, distension of bladder, and the development of end-stage hydronephrosis. In contrast, the heterozygous ($SM2^{+/-}$) mice appeared normal and reproduced well. In $SM2^{-/-}$ bladder smooth muscle the loss of SM2 myosin was accompanied by a concomitant down-regulation of SM1 and a reduced number of thick filaments. However, muscle strips from $SM2^{-/-}$ bladder showed increased contraction to K^+ depolarization or in response to M3 receptor agonist Carbachol. An increase of contraction was also observed in $SM2^{-/-}$ aorta. However, the $SM2^{-/-}$ bladder was associated with unaltered regulatory myosin light chain (MLC20) phosphorylation. Moreover, other contractile proteins, such as α-actin and tropomyosin, were not altered in $SM2^{-/-}$ bladder. Therefore, the loss of SM2 myosin alone could have induced hypercontractility in smooth muscle, suggesting that distinctly from SM1, SM2 may negatively modulate force development during smooth muscle contraction. Also, because $SM2^{-/-}$ mice develop lethal multiorgan dysfunctions, we propose this regulatory property of SM2 is essential for normal contractile activity in postnatal smooth muscle physiology.

contractility | myofilament | isoform-specific | gene-knockout

Smooth muscle myosin heavy chain (SMHC) is the motor protein that powers smooth muscle contraction (1–4). We have previously shown that a single SMHC gene encodes 4 different isoforms (SMA, SMB, SM1, and SM2), and their expression is restricted to the smooth muscle lineages, including visceral and vascular smooth muscle tissues (5–8). SMA and SMB isoforms differ by 7 aa in the S1 head region, and the SMB isoform containing the 7-aa insertion has higher myosin ATPase activity (9–11). By exon-specific gene targeting, we earlier reported that loss of SMB affects smooth muscle contractility and force velocity (12, 13). In a similar manner, alternate splicing at the 3′ end of the SMHC gene produces SM1 and SM2 isoforms; SM2 (200 kDa) contains a unique 9-aa sequence at the carboxyl terminus, whereas SM1 (204 kDa) has a 43-aa nonhelical tail region (5, 7). Interestingly, the C-terminal amino acid sequence that specifies SM1 and SM2 myosin isoform is highly conserved across all vertebrates.

During embryonic development, SM1 appears early by 10.5 days postcoitum, whereas SM2 appears late around birth (14). The ratio of SM2/SM1 has been found to be tissue-specific and altered in disease states. Decreased expression of SM2 has been found in primary pulmonary hypertension, neointimal smooth cells of injured or atherosclerotic vessels, and obstructive bladder disease (15–20). Also, there were studies suggesting that the ratio of SM1/SM2 contributes to the difference in contraction among smooth muscle tissues (21). However, the physiological relevance of each of these 2 COOH-terminal isoforms of SMHC to smooth muscle contractile property has not yet been clearly established. In this study, using an exon-specific gene-targeting strategy, we generated a mouse model specifically deficient in SM2 myosin and focused our studies on defining how the absence of SM2 affects filament structure and smooth muscle contraction.

Results

The Generation of SM2-Specific Knockout Mice. To generate a mouse model that is deficient in SM2 myosin but continues to express SM1 myosin, we used an exon-specific gene-targeting strategy as described (12). With this strategy, exon 41 of the SMHC gene (the region encoding 9 C-terminal amino acids plus a stop codon) and its flanking 5′ and 3′ splicing sequences were replaced with a neomycin-resistance cassette under the HSV-TK promoter in the reverse orientation in a targeting vector (Fig. 1). Successful targeting and germ-line transmission was confirmed by long-distance PCR analyses using primers specific for the WT and mutant alleles (data not shown). Both heterozygous ($SM2^{+/-}$) and homozygous ($SM2^{-/-}$) pups were delivered in an expected Mendelian ratio, which suggests that loss of SM2 does not result in embryonic lethality.

SM2 Deficiency Results in Multiorgan Dysfunction and Postnatal Lethality. The homozygous newborns had normal body size at birth; however, by day 20, the $SM2^{-/-}$ mice showed a significant decrease in body weight compared with the $SM2^{+/+}$ mice (8.88 ± 0.35 g vs. 15.61 ± 1.2 g; $P < 0.001$), and $\approx$50% of the homozygous mice died during the first 2 weeks. $SM2^{-/-}$ mice that survived beyond 2 weeks showed segmental distention of alimentary tract, retention of urine in renal pelvis or/and bladder, and development of end-stage hydronephrosis (Fig. 2*A*). All $SM2^{-/-}$ mice died within 4 weeks after birth, but the heterozygous mice appeared normal and reproduced well. We also found that the bladder body of peri-mortal $SM2^{-/-}$ mice was significantly distended (Fig. 2*B*). These data collectively suggest that SM2 myosin is essential for adult smooth muscle function and deficiency of SM2 myosin can lead to serious organ dysfunction as observed in bladder.

SM2 Deficiency Increases Smooth Muscle Contraction. Next, we determined how the deficiency of SM2 affected smooth muscle contraction. Isometric force development in bladder muscle

Author contributions: M.C., Y.Z., and M.P. designed research; M.C., Y.Z., S.V., and G.J.B. performed research; M.C., Y.Z., and M.P. analyzed data; and M.C., Y.Z., and M.P. wrote the paper.

The authors declare no conflict of interest.

This article is a PNAS Direct Submission.

[1]M.C. and Y.Z. contributed equally to this work.

[2]To whom correspondence should be addressed. E-mail: periasamy.1@osu.edu.

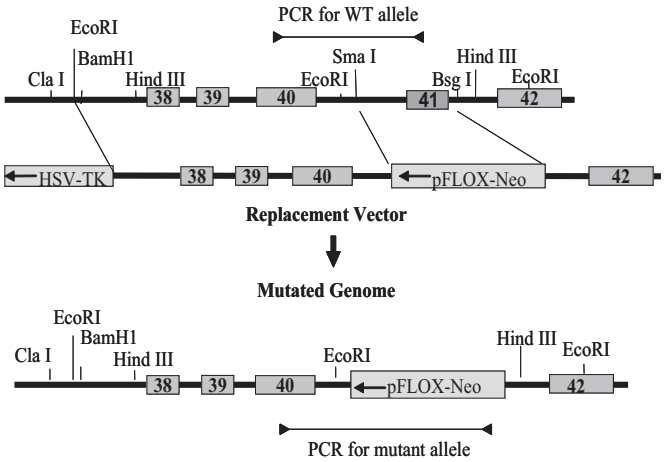

Fig. 1. SM2-specific gene-targeting strategy. Representation of exon 41-specific (SM2 isoform-specific) gene targeting strategy. Exon 41 of the SMHC gene and its flanking sequences were replaced with a neomycin gene in reverse orientation.

strips or aortic rings from 3- to 7-day-old neonate mice (a stage where overt pathology was not developed in $SM2^{-/-}$ bladder and aorta) was determined. As shown in Fig. 3*A*, whereas $SM2^{+/-}$ strips showed responses to K^+ comparable with that of $SM2^{+/+}$ mice, those of $SM2^{-/-}$ mice responded to K^+ with a significantly increased sustained phase of maximal contraction (689 ± 35 vs. 242 ± 26 mg or 84.3 ± 3.0% vs. 28.4 ± 2.8% of peak value at 60 mM K^+, $P < 0.001$; Fig. 3*A*) and a significantly reduced EC_{50} (concentration of K^+ to reach 50% of maximal contraction; 20.4 ± 0.4 vs. 42.9 ± 0.4 mM; $P < 0.001$). Similarly, in response to a submaximal (1 μM) concentration of Carbachol (a selective agonist of the M3 receptor that controls physiological bladder emptying), the $SM^{-/-}$ strips showed significantly enhanced contraction (105.6 ± 1.4% and 74.4 ± 3.8% vs. 49.3 ± 4.1% and 27.8 ± 5.0% in peak and sustained force, respectively; $P < 0.001$) compared with that of $SM^{+/+}$ (Fig. 3*B*). Moreover, aortic rings from $SM2^{-/-}$ null mice also showed increased contraction to the submaximal K^+ (30 mM) as compared with that of $SM2^{+/+}$ mice (86.2 ± 3.1% vs. 33.1 ± 5.7%, respectively, of the response caused by 60 mM K^+; $P < 0.01$; Fig. 3*C*). These results demonstrated that loss of SM2 myosin results in an increase in smooth muscle contractility.

Ca^{2+} Sensitivity, but Not Myosin Light Chain 20 (MLC20) Phosphorylation, Was Increased in $SM2^{-/-}$ Bladder. We next to tried to determine whether the increase in smooth muscle contractility was related to increased Ca^{2+} sensitivity of contractile apparatus in $SM2^{-/-}$ bladders by using skinned bladder strips. As shown in Fig. 4*A*, compared with that of $SM^{+/+}$ mice, the pCa^{2+}-force relationship in β-esin-permeabilized $SM2^{-/-}$ strips was significantly shifted to the left (EC_{50}: 0.93 ± 0.02 vs. 1.70 ± 0.15 μM; $P < 0.001$; Fig. 4*A*), which suggests that Ca^{2+} sensitivity of the contractile apparatus increased in the absence of SM2. It is well known that the phosphorylation of MLC20 initiates cross-bridge cycling and correlates with the force generation in smooth muscle contraction (22). Therefore, we further determined whether the phosphorylation status of MLC20 was altered in $SM2^{-/-}$ bladders. For this purpose, intact muscle strips were stimulated with 40 mM K^+, at which $SM2^{-/-}$ bladder developed maximal force, whereas $SM^{+/+}$ mice developed only 30–40% of maximal force. As shown in Fig. 4*B*, the ratios of phosphorylated to total MLC20 in both resting muscle and those treated with 40 mM K^+ were not significantly different between $SM2^{+/+}$ and

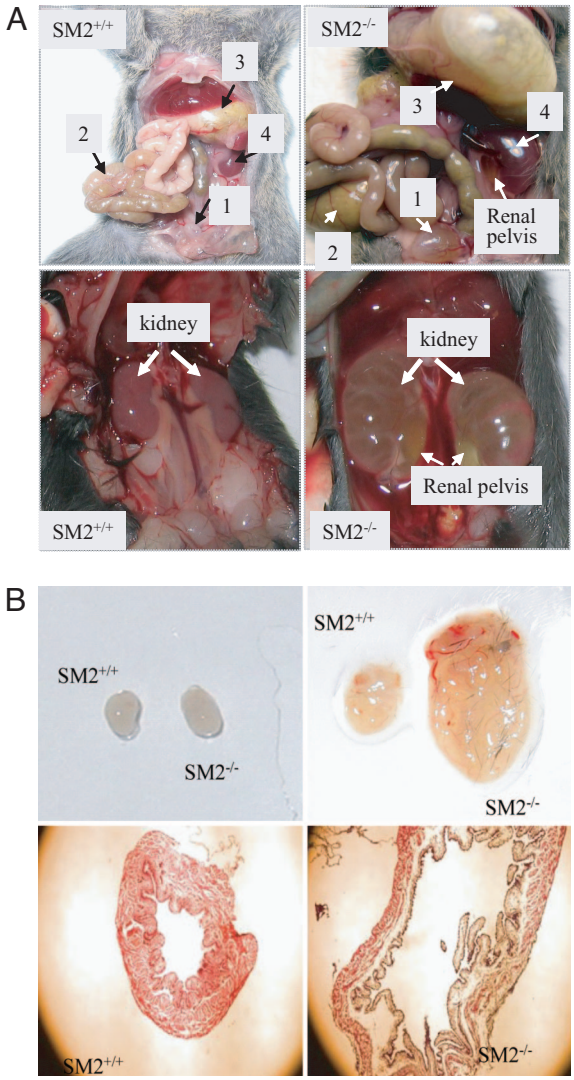

Fig. 2. Phenotype of $SM2^{-/-}$ mice. (*A*) (*Upper*) Comparison of bladder (square 1), alimentary tract (square 2) including stomach (square 3), and the kidney (square 4) in $SM^{+/+}$ and $SM^{-/-}$ mice (20 days). Note the retention of urine in the renal pelvis of $SM2^{-/-}$ kidney. (*Lower*) Development end-stage hydronephrosis with severe retention of urine in the renal pelvis in 25-day $SM2^{-/-}$ mice and kidneys in age-matched $SM2^{+/+}$ mice. (*B*) (*Upper*) Comparison of neonatal and peri-mortal $SM2^{-/-}$ with age-matched $SM^{+/+}$ bladders. (*Lower*) Histology (40×) of peri-mortal $SM2^{-/-}$ and age-matched $SM2^{+/+}$ bladders.

$SM2^{-/-}$ strips, suggesting that the loss of SM2 does not alter MLC20 phosphorylation status.

SM1 Myosin Level Was Decreased in SM2 Null Bladder. To understand how the loss of SM2 affects myosin and other contractile protein expression, total proteins were extracted from neonate bladders. Quantitative Western blot analysis showed that SM2 protein was absent in $SM2^{-/-}$ bladder as expected and was decreased by ≈20% in the $SM2^{+/-}$ bladder (Fig. 5*A*). Interestingly, there was a decrease in the level of SM1 in $SM2^{+/-}$ and $SM2^{-/-}$ bladder (≈27% and ≈56%, respectively; Fig. 5*A*). In addition, whereas nonmuscle myosin heavy chain B (NMHC-B) was not altered, the expression of NMHC-A was decreased by 42% in $SM2^{-/-}$ bladder (Fig. 5*A*). However, the levels of SM α-actin and SM α-tropomyosin, 2 key molecules that form thin filaments, were not altered in $SM2^{+/-}$ and $SM2^{-/-}$ bladder. These results

PHYSIOLOGY

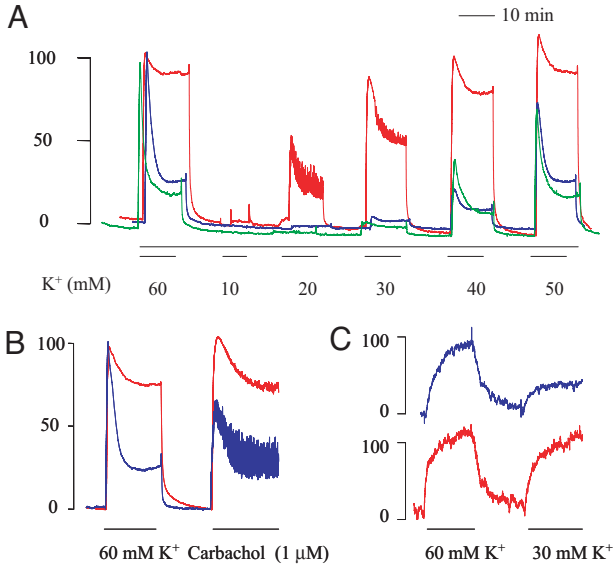

Fig. 3. Effect of SM2 deficiency on smooth muscle contraction. (*A* and *B*) Representative traces from 5–7 experiments showing the contraction to 60 mM K^+ with subsequent 10–50 mM K^+ (*A*) or 1 μM Carbachol (*B*) in $SM^{+/+}$ (blue), $SM2^{+/-}$ (green), or/and $SM2^{-/-}$ (red) bladders. (*C*) Representative traces from 4 experiments showing contraction of $SM^{+/+}$ (blue) and $SM2^{-/-}$ aortas (red) to submaximal contraction of K^+ (30 mM).

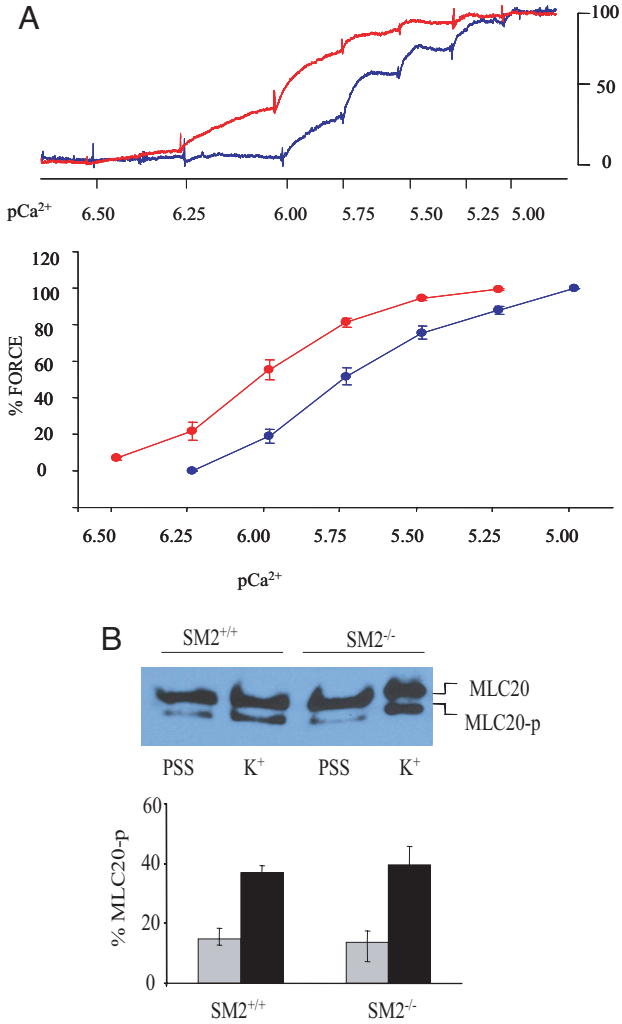

Fig. 4. Effect of SM2 deficiency on myofilament Ca^{2+} sensitivity and MLC20 phosphorylation. (*A*) Representative traces (*Upper*) and summary (*Lower*) of the responses induced by 0.3–10 μM Ca^{2+} in β-escin (50 μM)-permeabilized $SM^{+/+}$ (blue) and $SM2^{-/-}$ (red) strips. (*B*) Detection of phosphorylated and unphosphorylated MLC20 in resting (PSS) and 40 mM K^+ (K^+) stimulated smooth muscle of $SM2^{+/+}$ (gray bars) and $SM^{-/-}$ (black bars) bladders ($n = 4$).

demonstrated that SM2 deficiency selectively alter thick filament proteins in smooth muscle (Fig. 5*B*).

Thick Filament Density and Structure Are Altered in $SM2^{-/-}$ Mouse Bladder. To determine how changes in myosin heavy chain expression would affect thick filament formation, we performed electron microscopic analyses of $SM2^{-/-}$ bladder smooth muscle cells. As shown in Fig. 6, although the overall morphology of the smooth muscle cells was very similar, the number of thick filaments in a given field was significantly reduced in $SM2^{-/-}$ mice ($66 \pm 20.2/\mu m^2$ vs. $223.0 \pm 33.9/\mu m^2$ of $SM2^{+/+}$ mice, $P < 0.01$; Fig. 6). In addition, the diameters (x and y axis dimensions) of myosin filament cross-sections in $SM2^{-/-}$ bladder were significantly smaller than those of $SM2^{+/+}$ mice (10.2 ± 0.4 and 6.6 ± 0.3 nm vs. 15.3 ± 0.6 and 9.2 ± 0.4 nm, respectively, $n = 30$; $P < 0.001$; Fig. 6). These results demonstrated that SM2 deficiency not only decreases the density of thick filaments in smooth muscle, but also alters myofilament structure or architecture.

Discussion

We reported nearly 2 decades ago that SM1 and SM2 myosin isoforms that differ in the C terminus are generated by alternate splicing from a single gene (6); however, the functional relevance of these isoforms has not been understood. The goal of this study was to determine the role of SM2 myosin in smooth muscle contraction by using an exon-specific gene-targeting strategy. Loss of SM2 did not affect embryonic development; however, mice deficient in SM2 showed retarded growth and died postnatally by 4 weeks because of the development of multiorgan dysfunction, suggesting an essential role of SM2 in postnatal smooth muscle physiology. Also, our data from tissues of neonate mice suggest that smooth muscle without SM2 showed enhanced contractility, which further implies that SM2 myosin could possibly serve as an important regulator of smooth muscle contraction.

An important finding of this study is that smooth muscle tissues from $SM2^{-/-}$ mice responded with increased contraction, when treated with K^+ or M3 receptor agonist Carbachol. In addition, our experiments with β-escin-permeabilized muscle stripes showed that the Ca^{2+} sensitivity was increased in $SM2^{-/-}$ bladder. These data suggested that the absence of SM2 myosin enhanced the intrinsic contractility of contractile apparatus. However, the rate of MLC2 phosphorylation, the initiator of smooth muscle contraction, was very similar between the resting/K^+-stimulated $SM2^{-/-}$ and $SM2^{+/+}$ bladder strips, which argues that altered MLC phosphorylation status is not responsible for the increased contractility seen in SM2 null mice. Moreover, the thin filament contractile proteins, including SM α-actin and tropomyosin, were not significantly different between $SM2^{-/-}$ and WT bladder. Therefore, the loss of SM2 myosin itself was responsible for increased force development during smooth muscle contraction.

Another key observation of this study was that the deficiency of SM2 myosin resulted in a drastically reduced number of thick filaments in bladder smooth muscle cells. It should be noted that while the level of NMHC-B was unchanged, NMHC-A was in fact decreased in $SM2^{-/-}$ bladder, ruling out the possibility that the increased smooth muscle contraction in $SM2^{-/-}$ mice was caused by an up-regulation of nonmuscle myosin, which has been

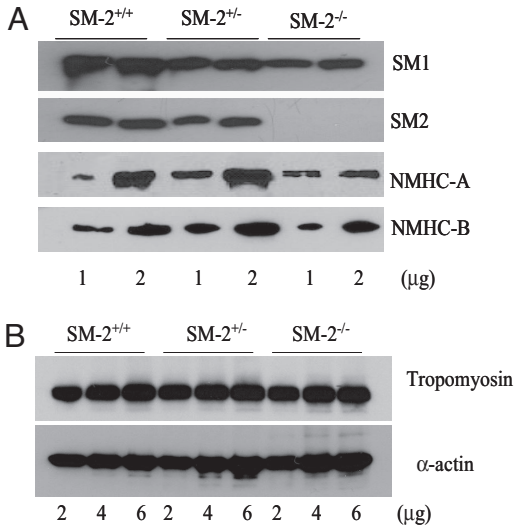

Fig. 5. Effect of SM2 deficiency on filament proteins. (*A*) Western blot analyses of SM1, SM2, and NMHC in mouse bladder. (*B*) Western blot analyses of α-actin and tropomyosin.

previously found to also form filaments and generate force in the absence of SMHC (23, 24). As a result, the increased contraction found in $SM2^{-/-}$ smooth muscle suggests that cells containing primarily SM1 myosin filaments (devoid of SM2) were able to produce an increased force even at a significantly lower thick filament density. However, bladder strips deficient in smooth muscle myosin (total SMHC gene deletion) were previously shown to produce a decreased contraction as compared with that of WT mice (23, 24). Therefore, SM2 appeared to function distinctly from the other SMHC isoform, SM1, and it was possible that the presence of SM2 myosin in $SM2^{+/+}$ mice might have negatively affected the force development during smooth muscle contraction.

The above findings were consistent with results of a previous study, in which the overexpression of SM1 or SM2 was found to increase or decrease mouse bladder smooth muscle contraction, respectively (21). However, in that study, biochemical evidence for the increase in SM1 or SM2 proteins was not shown. Interestingly, our current study further showed that in addition to the loss of SM2 SM1 myosin was decreased in $SM2^{-/-}$ or $SM2^{+/-}$ bladder. In addition, the $SM2^{+/-}$ bladder, which had a reduction in both SM2 and SM1 myosin, showed contractions that were comparable with those of $SM^{+/+}$ mice. These results suggest a dose-dependent effect of SM2 deficiency and that a partial loss of SM2 could be tolerated, possibly because of a concomitant down-regulation of SM1 myosin. Thus, the concomitant decrease of SM1 in $SM2^{+/-}$ and $SM2^{-/-}$ bladder could be considered as an adaptive response to maintain an appropriate ratio of SM1 and SM2, which appears to be essential for normal smooth muscle contractility.

Therefore, on the basis of the above findings, we propose that SM2 may act as a negative modulator of force development during smooth muscle contraction. Although the exact mechanism behind how this is accomplished needs to be defined, it should be emphasized that SM2 has a unique filament assembly property compared with SM1 isoform. Studies by Rovner *et al.* (25) showed that filaments formed by SM1 rod sequences were generally thin and stable, whereas those formed by SM2 appeared wide and branched. Also, our electron microscopic analyses of cross-sections showed that thick filaments in $SM2^{-/-}$ bladder were significantly smaller than those in $SM2^{+/+}$ bladder. Therefore, it is possible that the loss of SM2 myosin alters the overall architecture of thick filaments, resulting in greater force development during smooth muscle contraction. However, the exact mechanism for the increased force generation by filaments formed with only SM1 requires further investigation.

An intriguing finding of the current study was that in the presence of increased smooth muscle contractility $SM2^{-/-}$ mice showed severe dysfunction of several organs, including the development of segmental distention of alimentary tract, urinary retention, and end-stage hydronephrosis, which mimic complications developed in obstructive diseases. A possible explanation could be the differential distribution of SM2 among smooth muscle organs. For example, in the urethra, SM2 is more abundant than in the bladder (26). Thus, the ablation of SM2 could affect contractility differently among smooth muscle tissues and alter the functional coordination between organs involved in voiding and/or organ motility.

In summary, using a mouse model specifically deficient in SM2, we demonstrate that SM2 has a unique role and may negatively modulate the force development during smooth muscle contraction. Because $SM2^{-/-}$ mice died postnatally as a result of multiorgan dysfunction, we propose that SM2 is essential for maintaining normal contractile activities in postnatal smooth muscle physiology. However, future studies are needed regarding the molecular basis of SM2 in modulating force development during smooth muscle contraction.

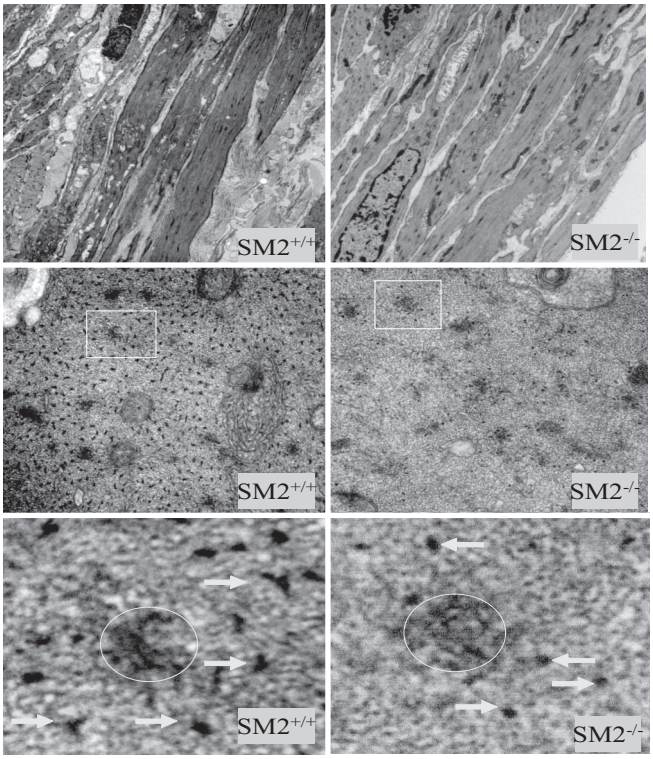

Fig. 6. Electron micrographs of bladder smooth muscle cells. (*Top*) Longitudinal section showing morphology of smooth muscle cells (6,000× magnification), (*Middle*) Cross-section of myosin filaments (68,000× magnification). (*Bottom*) Enlarged images (25×) of square areas indicated in *Middle*. Arrows point to the myosin thick filaments; circles indicate the locations of dense bodies.

Methods

Exon-Specific Gene Targeting. Genomic fragment of SM-MHC gene containing the 3′ region (20 kb) was isolated from a λ/129 mouse genomic library. Exon 41 and its 5′ and 3′ splicing sites (0.4 kb) were replaced with a neomycin-resistance cassette under the HSV-TK promoter in reverse orientation. The linearized construct was electroporated into mouse 129 embryonic stem cells.

PHYSIOLOGY

Clones resistant to neomycin were screened by long-distance PCR with primers specific for the WT allele and mutant allele. Targeted clones were injected into C57BL/6 blast cysts. Chimeric males were mated to B6 females, and the germ-line transmission of targeted allele was detected by long-distance PCR. $SM2^{-/-}$ mice were obtained by cross-breeding of $SM2^{+/-}$ mice.

Animals and Tissue Preparation. Neonate mice (3–7 days) were killed by decapitation, which was in accordance with National Institutes of Health guidelines and approved by the institutional animal care use committee at Ohio State University. Bladders were isolated and cut open, and the mucosa was removed by dissection under a binocular microscope. For the functional analyses, muscles from the front wall were cut transversally into 1- and 2-mm-long strips. The strips were tied with thread filaments to form a loop at both ends separated by a distance of 1 mm. In some experiments, thoracic aortas were also isolated and cut into 1-mm-long rings for functional analyses.

Analysis of Intact Smooth Muscle Contraction. Bladder muscle strips were attached with the loops to 2 tungsten wires in an organ bath (3 mL) filled with physiological salt solution (PSS) (27) maintained at 37 °C. One wire was fixed, and the other was connected to a force transducer (AE801; Holten). Tissues were set at 1.5 times resting length (at which length the contractile response to 60 mM K^+ was maximal and reproducible), and the contractions to the subsequent 10–50 mM K^+ or Carbachol (1 μM) were determined sequentially. The contraction of aortic rings was determined as described (27). Force was expressed as a percentage of peak value evoked by 60 mM K^+.

Myofilament Ca^{2+} Sensitivity. Bladder muscle strips were attached to the force apparatus as described above and set into 1.5 times resting length at room temperature. The strips were permeabilized with 50 μM β-esin (40 min) in Ca^{2+}-free cytosolic substitution solution (CSS) (28) and treated with 10 μM A23129 (10 min) in Ca^{2+}-free CSS. After washout, strips were exposed to free Ca^{2+}-containing CSS (0.3–10 μM). Force development at each Ca^{2+} point was expressed as a percentage of maximal contraction obtained with 10 μM Ca^{2+}.

Measurement of MLC20 Phosphorylation. Bladder muscle strips (1×2 mm^2) were placed in 37°C PSS or 40 mM K^+ for 5 min, and the reactions were stopped with 90% acetone, 10% trichloroacetic acid, and 10 mM DTT chilled at −80°C. Proteins were extracted, separated on Urea/glycerol gel (with the amount adjusted to achieve similar total MLC20 content between $SM2^{+/+}$ and $SM2^{-/-}$ mice), and transferred onto a nitrocellulose membrane as described (28). Phosphorylated and unphosphorylated MLC20 were probed with anti-MLC20 antibody (Sigma) as in Western blot analyses.

Analyses of Protein Expression. Protein expression was analyzed by SDS/PAGE and immunoblotting as described (12). Briefly, crude myofibril proteins isolated from bladder muscle were separated by using SDS/PAGE (5% for SM2 and SM1; 10% for α-actin and tropomyosin) and transferred to a nitrocellulose membrane. Proteins were sequentially probed with their respective first and secondary antibodies. Anti-SM1 and Anti-SM2 antibodies were kindly provided by A. F. Martin (University of Illinois Medical School, Chicago). Anti-α-actin and anti-MLC20 antibodies were purchased from Sigma. Anti-NMHC antibodies (A and B) were purchased from Covance. Band densities were quantified and analyzed with a Biochemi System (UVP).

Electron Microscopic Examination. The bladders were expanded in situ and fixed with 4% glutaraldehyde in 0.1 M phosphate buffer (pH 7.2). Strips cut from the treated bladders were further postfixed in 2% OsO_4 for 2 h at room temperature, and contrasted in saturated uranyl acetate for 4 h at 60 °C. Samples were embedded in Epon 812 and cut into sections, which were stained with uranyl acetate and lead. Images were detected and photographed with an electron microscope (EM 410; Philips Electron Optics). The number of thick filaments was counted and expressed in counts per μm^2. In addition, the diameters of myosin thick filaments cross-section (both *x* and *y* axis) in chosen fields were measured by using image analysis software (Scion Image, version 4.0.2).

Statistics. For statistical evaluation, values were presented as mean ± SE. Comparison of 2 means was performed by unpaired Student's *t* test. When >2 means were compared, 1-way or 2-way ANOVA followed by Dunnett's or Bonferroni's post hoc test was used. $P < 0.05$ was considered to be statistically significant.

ACKNOWLEDGMENTS. We thank Drs. Sumei Liu and Jackie Wood for expert help with tissue morphology. This work was supported by National Institutes of Health Grant HL 38355-17 (to M.P.). M.C. was supported by an American Heart Association Postdoctoral Fellowship Grant (Ohio Valley), and Y.Z. was supported by an American Heart Association Scientist Development Grant and a Davis Heart and Lung Institute Junior Investigator Award.

1. Rovner AS, Murphy RA, Owens GK (1986) Expression of smooth muscle and nonmuscle myosin heavy chains in cultured vascular smooth muscle cells. *J Biol Chem* 261:14740–14745.
2. Murphy RA, Walker JS, Strauss JD (1997) Myosin isoforms and functional diversity in vertebrate smooth muscle. *Comp Biochem Physiol B Biochem Mol Biol* 117:51–60.
3. Loukianov E, Loukianova T, Periasamy M (1997) Myosin heavy chain isoforms in smooth muscle. *Comp Biochem Physiol B Biochem Mol Biol* 117:13–18.
4. Craig R, Woodhead JL (2006) Structure and function of myosin filaments. *Curr Opin Struct Biol* 16:204–212.
5. Nagai R, Larson DM, Periasamy M (1988) Characterization of a mammalian smooth muscle myosin heavy chain cDNA clone and its expression in various smooth muscle types. *Proc Natl Acad Sci USA* 85:1047–1051.
6. Nagai R, Kuro-o M, Babij P, Periasamy M (1989) Identification of two types of smooth muscle myosin heavy chain isoforms by cDNA cloning and immunoblot analysis. *J Biol Chem* 264:9734–9737.
7. Babij P, Periasamy M (1989) Myosin heavy chain isoform diversity in smooth muscle is produced by differential RNA processing. *J Mol Biol* 210:673–679.
8. Miano JM, Cserjesi P, Ligon KL, Periasamy M, Olson EN (1994) Smooth muscle myosin heavy chain exclusively marks the smooth muscle lineage during mouse embryogenesis. *Circ Res* 75:803–812.
9. Lauzon AM, *et al.* (1998) A 7-amino acid insert in the heavy chain nucleotide binding loop alters the kinetics of smooth muscle myosin in the laser trap. *J Muscle Res Cell Motil* 19:825–837.
10. Kelley CA, Takahashi M, Yu JH, Adelstein RS (1993) An insert of seven amino acids confers functional differences between smooth muscle myosins from the intestines and vasculature. *J Biol Chem* 268:12848–12854.
11. Rovner AS, Freyzon Y, Trybus KM (1997) An insert in the motor domain determines the functional properties of expressed smooth muscle myosin isoforms. *J Muscle Res Cell Motil* 18:103–110.
12. Babu GJ, *et al.* (2001) Loss of SM-B myosin affects muscle shortening velocity and maximal force development. *Nat Cell Biol* 3:1025–1029.
13. Babu GJ, *et al.* (2004) Isoform switching from SM-B to SM-A myosin results in decreased contractility and altered expression of thin filament regulatory proteins. *Am J Physiol* 287:C723–C729.
14. White SL, Zhou MY, Low RB, Periasamy M (1998) Myosin heavy chain isoform expression in rat smooth muscle development. *Am J Physiol* 275:C581–C589.
15. Wang ZE, Gopalakurup SK, Levin RM, Chacko S (1995) Expression of smooth muscle myosin isoforms in urinary bladder smooth muscle during hypertrophy and regression. *Lab Invest* 73:244–251.
16. Cher ML, Abernathy BB, McConnell JD, Zimmern PE, Lin VK (1996) Smooth-muscle myosin heavy-chain isoform expression in bladder-outlet obstruction. *World J Urol* 14:295–300.
17. DiSanto ME, *et al.* (2003) Alteration in expression of myosin isoforms in detrusor smooth muscle following bladder outlet obstruction. *Am J Physiol* 285:C1397–C1410.
18. Packer CS, Roepke JE, Oberlies NH, Rhoades RA (1998) Myosin isoform shifts and decreased reactivity in hypoxia-induced hypertensive pulmonary arterial muscle. *Am J Physiol* 274:L775–L785.
19. Aikawa M, *et al.* (1993) Human smooth muscle myosin heavy chain isoforms as molecular markers for vascular development and atherosclerosis. *Circ Res* 73:1000–1012.
20. Itoh S, *et al.* (2002) Importance of NAD(P)H oxidase-mediated oxidative stress and contractile type smooth muscle myosin heavy chain SM2 at the early stage of atherosclerosis. *Circulation* 105:2288–2295.
21. Martin AF, *et al.* (2007) Expression and function of COOH-terminal myosin heavy chain isoforms in mouse smooth muscle. *Am J Physiol* 293:C238–C245.
22. Somlyo AP, Somlyo AV (2003) Ca^{2+} sensitivity of smooth muscle and nonmuscle myosin II: Modulated by G proteins, kinases, and myosin phosphatase. *Physiol Rev* 83:1325–1358.
23. Morano I, *et al.* (2000) Smooth-muscle contraction without smooth-muscle myosin. *Nat Cell Biol* 2:371–375.
24. Lofgren M, Ekblad E, Morano I, Arner A (2003) Nonmuscle myosin motor of smooth muscle. *J Gen Physiol* 121:301–310.
25. Rovner AS, Fagnant PM, Lowey S, Trybus KM (2002) The carboxyl-terminal isoforms of smooth muscle myosin heavy chain determine thick filament assembly properties. *J Cell Biol* 156:113–123.
26. Hypolite JA, *et al.* (2001) Regional variation in myosin isoforms and phosphorylation at the resting tone in urinary bladder smooth muscle. *Am J Physiol* 280:C254–C264.
27. Zhou Y, Dirksen WP, Babu GJ, Periasamy M (2003) Differential vasoconstrictions induced by angiotensin II: Role of AT1 and AT2 receptors in isolated C57BL/6J mouse blood vessels. *Am J Physiol* 285:H2797–H2803.
28. Zhou Y, Hirano K, Sakihara C, Nishimura J, Kanaide H (1999) NH_2-terminal fragments of the 130-kDa subunit of myosin phosphatase increase the Ca^{2+} sensitivity of porcine renal artery. *J Physiol (London)* 516:55–65.